OXFORD GENETICS

GENETICS, 2026, iyag105
https://doi.org/10.1093/genetics/iyag105
Advance Access Publication Date: 24 April 2026
Investigation

Prevalence, distribution, and mechanisms of genetic dominance in the yeast mating pathway

M. Grace Allen, Artemiza A. Martínez, Gregory I. Lang *

Department of Biological Sciences, Lehigh University, Bethlehem, PA 18015, United States

*Corresponding author: Department of Biological Sciences, Lehigh University, Bethlehem, PA 18015, United States. Email: glang@lehigh.edu

The proportion of mutations that are dominant is a fundamental genetic parameter affecting the rate of adaptation, the efficacy of selection, and the maintenance of variation in populations. Yet, estimates for this parameter vary greatly. Here we directly quantify the rates and genetic targets of dominant and recessive mutations in the yeast mating pathway by performing parallel genetic screens in haploid (*MAT***a**) and diploid (*MAT***a**/**a**) yeast. We find that ~1% of alpha-factor-resistant mutations are dominant. We sequenced 95 alpha-factor-resistant mutants to determine the genetic architecture of dominant and recessive mutations. We find recessive mutations throughout the mating pathway; however, dominant mutations are concentrated in 3 genes: *STE4*, *GPA1*, and *CLN3*. Finally, we investigate the mechanism of genetic dominance in each of these genes. This work sheds light on the prevalence and molecular basis of genetic dominance in a model eukaryotic signal transduction pathway.

Keywords: genetic dominance; mutation rate; *Saccharomyces cerevisiae*; mating pathway; Yeast2026

Introduction

Most loss-of-function mutations are recessive. A systematic analysis in yeast found that only ~3% of gene deletions show a measurable phenotype when heterozygous (Deutschbauer et al. 2005). Dominant mutations, therefore, must act through specific mechanisms of action, for example, constitutive activation of a protein or disruption of a protein complex. Classic mutagenesis studies suggest that less than 10% of spontaneous mutations are dominant (Wilkie 1994). However, more recent estimates from deep mutational scanning studies suggest that the fraction of dominant mutations may be as high as a third of all possible mutations (Padhy et al. 2023; Flynn et al. 2024). Discrepancies in these estimates could be due to specifics of the gene or phenotype under study or the criteria used to assess dominance. One approach to determine the proportion of mutations that are genetically dominant is to measure mutation rates in isogenic haploids and diploids, ideally in a way that samples many genetic targets using the same selection.

The yeast mating pathway is one of the best studied signal-transduction pathways (Herskowitz 1995; Alvaro and Thorner 2016). Signaling is initiated by the mating pheromone (α-factor or **a**-factor) which binds to the cognate receptor (Ste2 or Ste3 for *MAT***a** and *MAT*α cells, respectively). Pheromone binding activates a heterotrimeric G protein, which signals through a MAPK cascade, resulting in both a cell-cycle arrest and a transcriptional response (Bardwell 2005). Mutations that disrupt signaling can therefore be recovered as alpha-factor-resistant colonies, providing a simple selection on pathway function. While genetic screens have been instrumental in identifying the components of the yeast mating pathway (Mackay and Manney 1974a, 1974b; Manney and Woods 1976; Hartwell 1980), all direct screens for mating mutants have been performed with haploid yeast, as true (*MAT***a**/α) diploids do not have an active mating pathway. Therefore, classic genetic screens for mating defects may have missed rare dominant mutations.

Here, we perform genetic screens to isolate alpha-factor resistance mutants from both isogenic haploid (*MAT***a**) and diploid (*MAT***a**/**a**) yeast strains to estimate the fraction of resistance mutations that are dominant and to identify the genes and mechanisms that generate dominance in this selection. We characterized 95 alpha-factor-resistant mutants by phenotyping and whole-genome sequencing to identify the underlying causative mutations. We find that ~1% of alpha-factor-resistant mutations are dominant. Unlike recessive alpha-factor resistance mutations that are distributed throughout the pathway, dominant mutations are concentrated in 3 genes: *STE4*, *GPA1*, and *CLN3*.

Materials and methods

Yeast strains and plasmids

Strains yGIL432 (haploid *MAT***a**) and yGIL1132 (diploid *MAT***a**/**a**) are derived from the W303 background. yGIL432 has the genotype *ura3*Δ::p*FUS1*::yeVenus *ade2-1*, *his3-11,15*, *leu2-3,112*, *trp1-1*, *CAN1*, *bar1*Δ::*ADE2*, *hml*Δ::*LEU2 GPA1*::NatMX. yGIL1132 is a homozygous diploid derivative of yGIL432. The only exception is at the *URA3* locus, which is heterozygous: *ura3*/*ura3*Δ::p*FUS1*::yeVenus. We assayed mating and **a**-factor production using mating-type testers yGIL355 (*MAT*α, *met4*Δ::KanMX) and yGIL617 (*MAT*α, *sst2*),

Received on 14 March 2026; accepted on 14 April 2026
© The Author(s) 2026. Published by Oxford University Press on behalf of The Genetics Society of America.
This is an Open Access article distributed under the terms of the Creative Commons Attribution-NonCommercial-NoDerivs licence (https://creativecommons.org/licenses/by-nc-nd/4.0/), which permits non-commercial reproduction and distribution of the work, in any medium, provided the original work is not altered or transformed in any way, and that the work is properly cited. For commercial re-use, please contact reprints@oup.com for reprints and translation rights for reprints. All other permissions can be obtained through our RightsLink service via the Permissions link on the article page on our site—for further information please contact journals.permissions@oup.com.

Downloaded from https://academic.oup.com/genetics/advance-article/doi/10.1093/genetics/iyag105/8662036 by Lehigh University user on 28 May 2026

respectively. We sporulated diploid *MAT***a**/**a** for tetrad dissections by transforming with the plasmid pGIL069, a *URA3* marked CEN/ARS plasmid with the *MAT*α mating-type information. Tetrad dissections were used to test whether alpha-factor resistance segregated 2:2, consistent with a single heterozygous causal mutation. We constructed *MAT***a**/**a** diploid derivatives of *MAT***a** alpha-factor-resistant clones by first complementing the sterile mutation using the appropriate plasmid from the MoBY ORF plasmid collection (Ho et al. 2009). These *MAT***a**/**a** derivatives were used as recessivity tests to determine whether alpha-factor-resistance mutations isolated in haploids remained resistant in a diploid context (Supplementary Fig. 3). We then crossed these strains to yGIL2345, a *MAT*α version of yGIL432 which has KanMX in place of NatMX at the *GPA1* locus and carrying pGIL088, a *URA3* marked plasmid with a galactose-inducible *HO* and the *SpHIS5* gene under control of the *STE2* promoter. We selected for diploids on YPD+G418+ClonNat. Following mating-type switching, we selected *MAT***a**/**a** clones on SC-his plates. Finally, we eliminated the plasmids by counter-selecting on 5FOA.

Measuring mutation rates

We measured mutations rates using Luria–Delbrück fluctuation assays as described previously (Lang and Murray 2008; Lang 2018) with minor adjustments. We grew strains in low-glucose (0.2%) YPD medium using 10 or 100 μl culture volumes for haploid and diploids, respectively. After 1 day of growth, we brought the cultures up to 100 μl, if necessary, and spot-plated onto YPD medium containing alpha-factor (10 μg/ml). For each assay, we initiated 96 replicate cultures, 24 of which were used to estimate the number of cells per culture and 72 of which were plated to determine the distribution of the number of alpha-factor-resistant cells per culture. We analyzed the data from fluctuation assays using the Ma-Sandri-Sarkar maximum likelihood method in which the data are fit to a model of the Luria–Delbrück distribution based upon a single parameter m, the expected number of mutation events per culture (Sarkar et al. 1992). We determined the cell number by hemocytometer and calculated mutation rate using the equation $\mu = m/N$, where N is the average number of cells per culture (approximately equal to the number of cell divisions per culture since the initial inoculum is much smaller than N). We assigned 95% confidence intervals on m and μ using equations 24 and 25 from (Rosche and Foster 2000). For downstream analyses, we selected 95 independent alpha-factor-resistant clones (47 diploid and 48 haploid alpha-factor-resistant clones), which were arrayed in a 96-well plate. To maintain consistency across phenotyping, genetic analysis, and sequencing, we retained the original plate-position identifiers throughout the study; haploid clones occupied columns 1 to 6 and diploid clones occupied columns 7 to 12.

Whole-genome sequencing

We sequenced alpha-factor-resistant clones as well as alpha-factor-resistant and sensitive pools using 150 nt × 150 nt paired-end sequencing on an Illumina HiSeq 2500 at the Sequencing Core Facility within the Lewis-Sigler Institute for Integrative Genomics at Princeton University. Raw reads were trimmed using trimmomatic/0.36 (Bolger et al. 2014) using PE -phred33 parameter. Each sample was aligned to the complete and annotated W303 genome (Matheson et al. 2017) using BWA-MEM, v.0.7.15 (Li and Durbin 2009). Variants were identified using FreeBayes/1.1.0 (Garrison and Marth 2012), using default parameters. Variants common to all samples were filtered using the VCFtools/0.1.15 vcf-isec function (v.0.1.12b). Individual VCF files were annotated using SnpEff/5.0 using -formatEff flag (Cingolani et al. 2012). We verified the variant calling by viewing individual mutations using Integrated Genome Viewer (Broad Institute). Copy number variants (CNVs) were identified using ControlFREEC version 11.5 (Boeva et al. 2012). All the text outputs were merged into one data frame to remove all the common calls. We filtered CNV calls by excluding variants that were called more than 10 times, were less than 5 kb, or were located within 5 kb of a telomere or centromere. CNVs and aneuploidies were corroborated by visual inspection of chromosome coverage plots created in R. Briefly, we used samtools-depth to calculate per-site depth from the sorted-bam files. We divided the median chromosome coverage by the median genome-wide coverage using non-overlapping 1,000 bp window size and 500 nt step size. The total coverage of the genome was normalized to 1 or 2 for haploid or diploid clones, respectively.

Phenotypic assays

Supplementary Fig. 1 shows a schematic of the experimental workflow. In addition to whole genome sequencing and genetic tests, the alpha-factor-resistant clones were assayed for relevant phenotypes. Strains yGIL432 and yGIL1132 contain the yEVenus reporter under the control of the *FUS1* promoter downstream of the yeast mating pathway. Using flow cytometry, we assayed basal expression or induced expression following 4 h in 10 μg/ml alpha factor (Supplementary Fig. 1b). We assayed **a**-factor production by the ability to produce a halo on a lawn of the halo tester strain yGIL617 (Supplementary Fig. 1c and Supplementary Fig. 2). We scored alpha-factor hypersensitivity if a strain failed to show robust growth in the presence of pheromone produced by the halo-tester lawn (Supplementary Fig. 1c and Supplementary Fig. 2). We assessed mating ability by scoring growth on minimal medium following mating between yGIL432 or yGIL1132 and mating tester strain, yGIL335.

To call basal signaling, we set a threshold of 425 fluorescence units, which separates the control strains that lack basal signaling from the control strains that have basal signaling (Supplementary Table 1). To identify strains that show alpha-factor induced signaling, we set the threshold at 10,000 fluorescence units, which again separates the inducible and non-inducible control strains (Supplementary Table 1). To determine intermediate phenotypes, we performed a statistical outlier analysis in Matlab. For basal expression, we identified 4 outliers whose basal expression was higher than expected (Fig. 2, Supplementary Table 1); we indicate these by "++" in Fig. 2. For induced expression, we identified 2 strains that show intermediate levels of induction (Fig. 2, Supplementary Table 1); we indicate these strains by "+/−" in Fig. 2. For clustering we used binary values (0,1) for (−, +). We set "+/−" equal to 0.5 and "++" equal to 1.5.

Results and discussion

One percent of the mutations that interfere with the mating pathway are dominant

To determine the relative abundance of dominant and recessive mutations that affect the yeast mating pathway, we performed fluctuation assays to measure the rate of alpha-factor resistance mutations in haploid *MAT***a** and diploid *MAT***a**/**a** backgrounds (Table 1). We find that the mutation rate to alpha-factor resistance in our haploid strain is 2.28×10^{-6} per genome per generation (1.75×10^{-6}, 2.86×10^{-6}, 95% CI). This assay was performed in an *hml*αΔ strain to prevent expression of the *MAT*α information due to mating-type switching or loss of silencing. Previous

Downloaded from https://academic.oup.com/genetics/advance-article/doi/10.1093/genetics/iyag105/8662036 by Lehigh University user on 28 May 2026

Table 1. Mutation rates to alpha-factor resistance.

Strain	Ploidy	Relevant genotype	Mutation rate	95% CI	Fold relative to yGIL432
yGIL104	Haploid	*MAT***a** *HML*α	5.86×10^{-6}	5.46×10^{-6}–6.28×10^{-6}	2.57
yGIL432	Haploid	*MAT***a** *hml*α*Δ*	2.28×10^{-6}	1.75×10^{-6}–2.86×10^{-6}	1.00
yGIL1132	Diploid	*MAT***a**/**a** *hml*α*Δ*/*hml*α*Δ*	3.10×10^{-8}	1.31×10^{-8}–5.41×10^{-8}	0.01

Table 2. Segregation patterns for alpha-factor-resistant diploid clones.

Clone	Mutations	Causative mutation	Segregation patterns	
			Viability	αF resistance
Diploid A07	1	*CLN3*	4:0	Mixed (2:2, 3:1)
Diploid A08	2	*CLN3*	Mixed (4:0, 3:1, 2:2)	Mixed (20/27 αFR)
Diploid A12	0		4:0	0:4
Diploid B07	1	*GPA1*	4:0	2:2
Diploid B08	2		4:0	2:2
Diploid B09	2	*GPA1*	4:0	2:2
Diploid B10	2	*GPA1*	4:0	2:2
Diploid B12	1		4:0	2:2
Diploid C08	1	*GPA1*	4:0	2:2
Diploid C09	3	*STE4*	4:0	2:2
Diploid C10	1	*STE4*	4:0	2:2
Diploid C11	1	*CLN3*	4:0	Mixed (3:1, 2:2)
Diploid D08	2	*GPA1*	2:2	2:2
Diploid D09	3	*STE11*	2:2	2:0
Diploid D10	2	*GPA1*	4:0	2:2
Diploid D12	2		4:0	2:2
Diploid E10	2	*STE4*	4:0	2:2
Diploid F12	0		2:2	2:2
Diploid G09	2		4:0	0:4
Diploid G11	3		2:2	2:2

measurements of the rate of alpha-factor resistance in an *HML*α strain are 2-fold higher (Table 1), consistent with estimates of mating type switching at a rate of ~10^{-6} per genome per generation (Hicks and Herskowitz 1976; Strathern and Herskowitz 1979). We find that the mutation rate to alpha-factor resistance in *MAT***a**/**a** diploids is 3.10×10^{-8} per genome per generation (1.31×10^{-8}, 5.41×10^{-8}, 95% CI), 2 orders of magnitude lower than the rate in haploid cells. This suggests that ~1.4% of mutations that confer alpha-factor resistance are dominant (0.4% to 2.3%, 95% CI), much lower than the estimate of ~30% from systematic studies of deep mutational scanning (Padhy et al. 2023; Flynn et al. 2024) and lower than the estimate of <10% from surveys of spontaneous mutations (Wilkie 1994).

Most alpha-factor-resistant diploid clones harbor a single dominant alpha-factor resistance mutation

We selected 47 diploid and 48 haploid alpha-factor-resistant clones for further study. We performed tetrad dissections on 20 of the diploid clones to determine the segregation pattern of alpha-factor resistance (Table 2). Most clones showed the expected segregation pattern of 2:2 for alpha-factor resistance. Three clones (Diploid A07, A08, and C11) showed mixed segregation patterns for spore viability and alpha-factor resistance. These clones were later found to harbor mutations in *CLN3* (Table 2) which interacts with *IME1*, the master regulator of meiosis (Colomina et al. 1999). One clone (Diploid D09) produced only alpha-factor-resistant spores, consistent with a homozygous mutation, whereas 2 clones (Diploid A12 and G09) produced only alpha-factor sensitive spores. To determine whether haploid clones carry recessive alpha-factor resistance mutations, we backcrossed 4 haploid clones (Haploid B01, D02, D03, and G03) to a wild-type strain and gene-converted the *MAT* locus to assay alpha-factor sensitivity (Supplementary Fig. 3). All 4 backcrossed haploid clones are sensitive to alpha-factor. Combined, these experiments are consistent with single dominant alpha-factor-resistant mutations arising in the *MAT***a**/**a** diploid background and recessive alpha-factor-resistant mutations in the haploid *MAT***a** background.

Recessive and dominant mutations affect different parts of the mating pathway

We sequenced all 47 diploid and 48 haploid alpha-factor-resistant clones, as well as pooled sensitive and resistant spores from tetrad dissections of diploid clones C08, C09, C10, D08, D09, and D10. We find a similar number of mutations in the haploid and diploid alpha-factor-resistant clones: 1.50 mutations (range of 0 to 5) for the haploid clones and 1.45 mutations (range of 0 to 3) for the diploid clones. For 45 of the 48 haploid clones and 33 of the 47 diploid clones, we could unambiguously identify the causative alpha-factor resistance mutation in a gene associated with the yeast mating pathway or cell-cycle progression. In all cases but one, these mutations were non-synonymous. The only exception is a mutation upstream of the *STE4* gene in the haploid clone G05; this mutation appears to create an out-of-frame start codon 50 bp upstream of the annotated start site and is therefore predicted to behave as a null mutation. Among diploid clones, 26 of the 33 candidate causative mutations are heterozygous. This result is consistent with the tetrad dissections, which showed 2:2 (or close to 2:2) segregation of alpha-factor resistance in 17 of the 20 diploid clones (Table 2).

Excluding the homozygous mutations in the diploid clones, alpha-factor resistance mutations in haploids and diploids affect distinct parts of the yeast mating pathway (Fig. 1). Recessive mutations (those arising in haploids or present as homozygous in the diploid) are found throughout the pathway, with the highest enrichment in the MAPK cascade (*STE11*, *STE7*, and *STE5*) and the transcription factor (*STE12*). In contrast, dominant mutations are found concentrated in the Gα and Gβ subunits (encoded by *GPA1* and *STE4*, respectively) as well as the cyclin gene, *CLN3*.

Some diploid clones contain additional recessive mutations

In diploid clones, we observed 7 cases of loss of heterozygosity (LOH)—*STE2* in A09, B11, G10, H11; *STE5* in H08; and *STE11* in D09 and F07—and at least 4 clones (A09, B11, G10, G11) that harbor one or more aneuploidies (Supplementary Dataset 1 and Supplementary Fig. 4). The number of homozygous mutations is somewhat surprising given that only ~20 generations of growth occurred prior to plating on selective medium and homozygous mutations require a 2-step process (mutation followed by LOH). Two homozygous mutations occurred in *STE11*, which lies distal to the rDNA repeat on Chromosome XII, a known hotspot for mitotic recombination (Marad et al. 2018). Four homozygous

Downloaded from https://academic.oup.com/genetics/advance-article/doi/10.1093/genetics/iyag105/8662036 by Lehigh University user on 28 May 2026

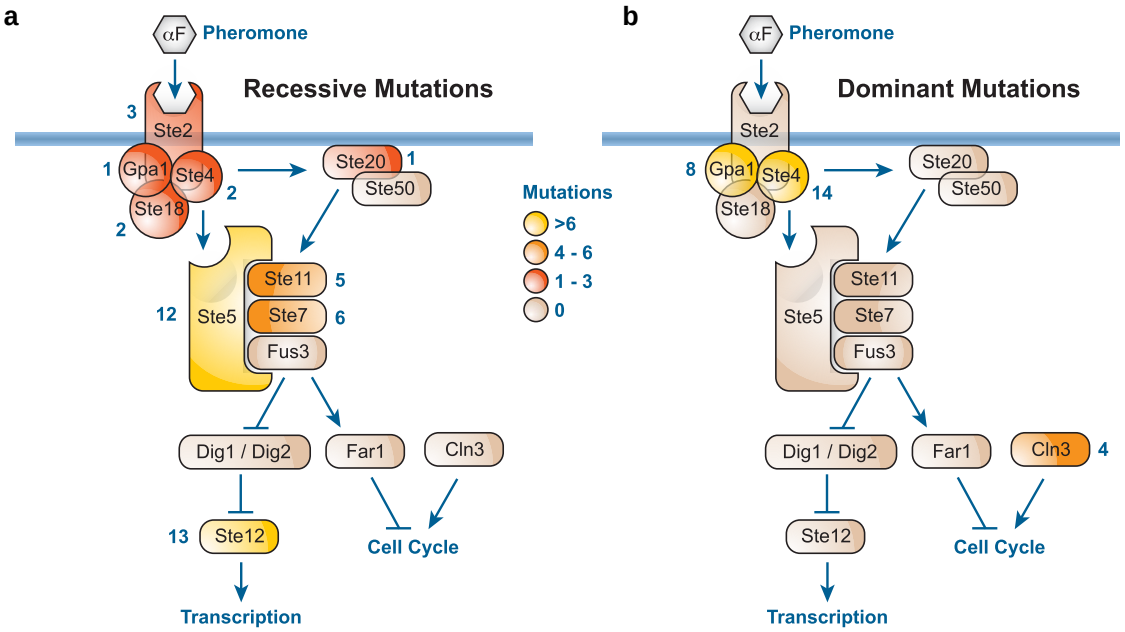


Fig. 1. Recessive and dominant mutations affect different parts of the mating pathway. Schematic of the yeast mating pathway showing the number of times each gene was identified as the putative alpha-factor-resistant mutation in the *MAT***a** (recessive) and *MAT***a**/**a** (dominant) genetic screens, respectively. a) Recessive mutations are found throughout the mating pathway. b) Dominant mutations are found only in the Gα and Gβ subunits (encoded by *GPA1* and *STE4*, respectively) as well as the cyclin gene, *CLN3*. Seven mutations from the *MAT***a**/**a** screen that underwent loss-of-heterozygosity are not shown.

mutations in *STE2* on Chromosome VI were accompanied by loss of Chromosome VI and Chromosome I (Supplementary Fig. 4). Given that about 7 of the 47 alpha-factor resistance mutations in the diploids are recessive, the mutation rate to dominant resistance (2.64×10^{-8}) is slightly less than the mutation rate to alpha-factor resistance in diploids (3.10×10^{-8}, Table 1).

Homozygous mutations and aneuploidies also explain some of the unexpected segregation patterns (Table 2). Most clones were consistent with a single, dominant alpha-factor-resistant mutation: 4-spore viable tetrads segregating 2:2 alpha-factor resistance. However, 4 of the 20 clones showed 2:2 segregation for viability, indicating that, besides the resistant mutation, these clones also harbor a recessive lethal mutation, which could arise from a point mutation or the loss of an entire chromosome. For diploid clone D09, we observe 2:2 segregation of viability and 2:0 segregation of alpha-factor resistance. This clone has a normal karyotype, a homozygous *STE11* mutation, and heterozygous missense mutation in *RIB4* and *UBC7* (Supplementary Dataset 1). Neither *RIB4* nor *UBC7* is annotated as essential genes in the Saccharomyces Genome Database. To identify the recessive lethal mutation in clone D09, we sequenced the pooled viable spores. We find that, while the *UBC7* mutation is present in the viable spores, the *RIB4* mutation is absent, suggesting that this *RIB4* mutation may be lethal in our strain background.

Dominant and recessive alpha-factor resistance mutations fall into distinct phenotypic clusters

We measured phenotypes associated with mating ability for all haploid and diploid alpha-factor-resistant mutants, including basal and induced expression using a p*FUS1*-yEVenus reporter, **a**-factor production, and mating ability. We also assessed pheromone sensitivity in 2 ways: by replating on YPD+alpha factor and by spotting on a lawn of *MAT*α cells (Fig. 2). Clustering the phenotypes produces expected relationships: basal expression clusters with a-factor production and induced expression clusters with mating ability. Interestingly, 22 of the 47 diploid clones initially isolated on YPD+alpha factor arrested when retested, despite most of them having a confirmed heterozygous mutation in the mating pathway, suggesting reduced penetrance of dominant resistance mutations.

Resistant clones formed 3 main clusters. Cluster 1 contains haploid clones harboring recessive null mutations in the pathway; these clones showed strong mating defects and lack detectable basal expression. Mutations in Cluster 1 occurred throughout the pathway but are particularly enriched in the MAPK pathway genes *STE11* (5/44), *STE7* (6/44), *STE5* (12/44) and the transcription factor gene *STE12* (13/44). Cluster 2 includes both haploid and diploid clones with intermediate phenotypes: clones show basal expression through the pathway but lack either induced expression or mating ability. Mutations in Cluster 2 tend to fall in the alpha-factor receptor gene *STE2* (6/19), or the Gα subunit gene, *GPA1* (6/19). Cluster 3 contains diploid clones with modest effects on mating-related phenotypes; mutations were concentrated in the Gβ subunit gene, *STE4* (14/32), and the G1 cyclin gene, *CLN3* (4/32).

Dominant mutations in *GPA1* and *CLN3* are gain-of-function

The identities and patterns of mutations in *GPA1* and *CLN3* imply specific molecular mechanisms for dominant alpha-factor-resistant mutations. Dominant *GPA1* mutations cluster in 2 regions. The first region is in the GTP binding domain. Prior work showed that mutations at residues Gly322, Arg327, and Glu364 (the "G-R-E motif") in Gpa1 (Gα) stabilize the GDP-bound configuration, locking the protein in the inactive state and preventing Ste4/Ste18 (Gβγ) release (Knight et al. 2021). Adjacent mutations (Gln323Lys and Asn233Asp) produce a similar phenotype (Wu et al. 2004). Consistent with this, we observe 3 substitutions at Gly322 (Gly322Val, Gly322Arg, Gly322Glu) and one at Glu364

Downloaded from https://academic.oup.com/genetics/advance-article/doi/10.1093/genetics/iyag105/8662036 by Lehigh University user on 28 May 2026

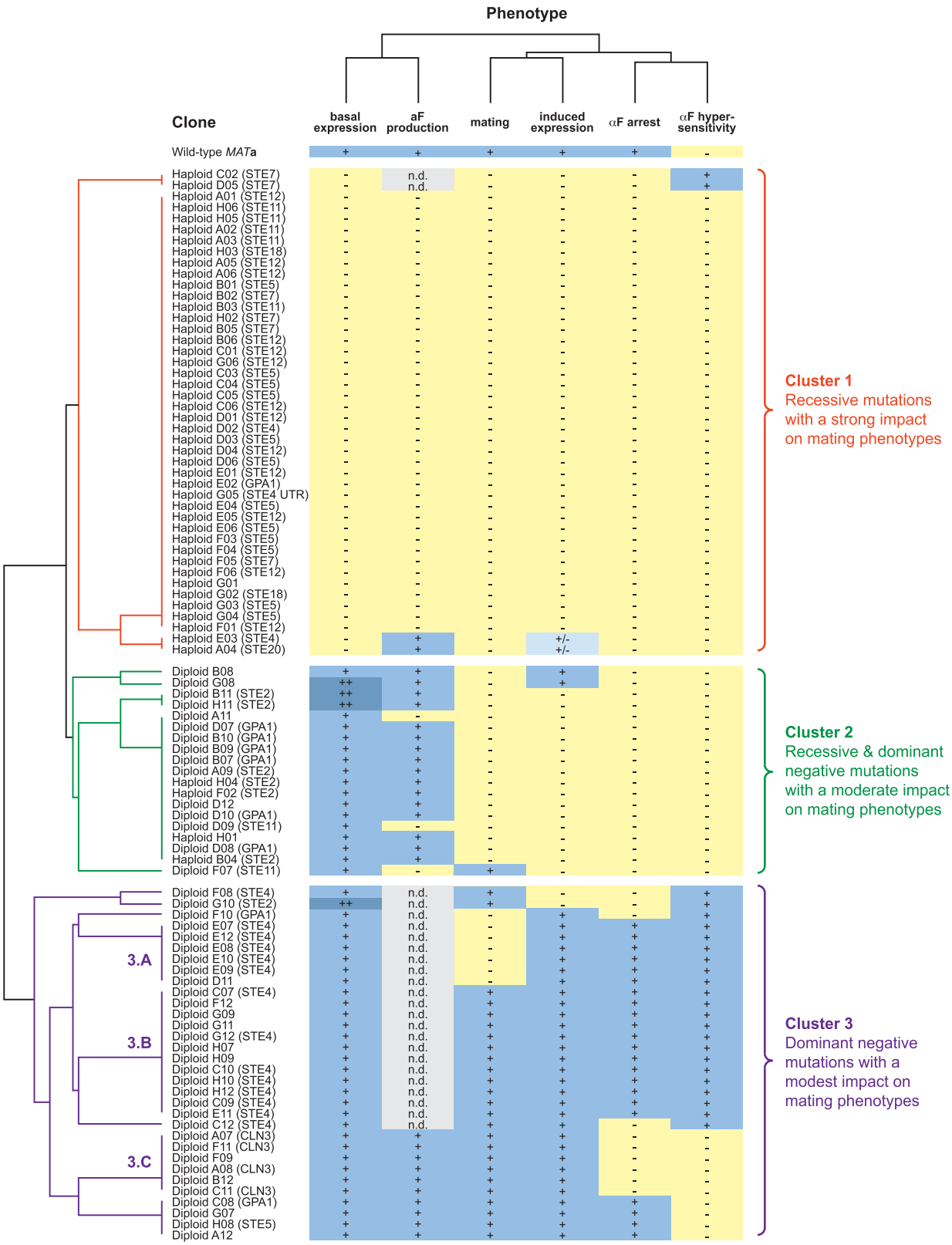


Fig. 2. Diverse phenotypes among sterile mutants. We measured 6 phenotypes associated with mating ability for all haploid and diploid alpha-factor-resistant mutants. All phenotypes were binary, with a few exceptions. We were unable to assay **a**-factor production for strains that were hypersensitive to alpha-factor. Several strains displayed higher than WT basal expression (++), and some strains displayed intermediate levels of induced expression (+/–). We clustered the data by both clone and by phenotype.

(Glu364Lys; Fig. 3). While we do not find mutations at Arg327, we do observe a mutation at an adjacent, and well-conserved, arginine residue (Arg324Leu).

A second group of dominant *GPA1* mutations cluster in the C-terminal α5 helix, which is the primary point of contact between Gpa1 and the Ste2 receptor (Velazhahan et al. 2021). Missense

Downloaded from https://academic.oup.com/genetics/advance-article/doi/10.1093/genetics/iyag105/8662036 by Lehigh University user on 28 May 2026

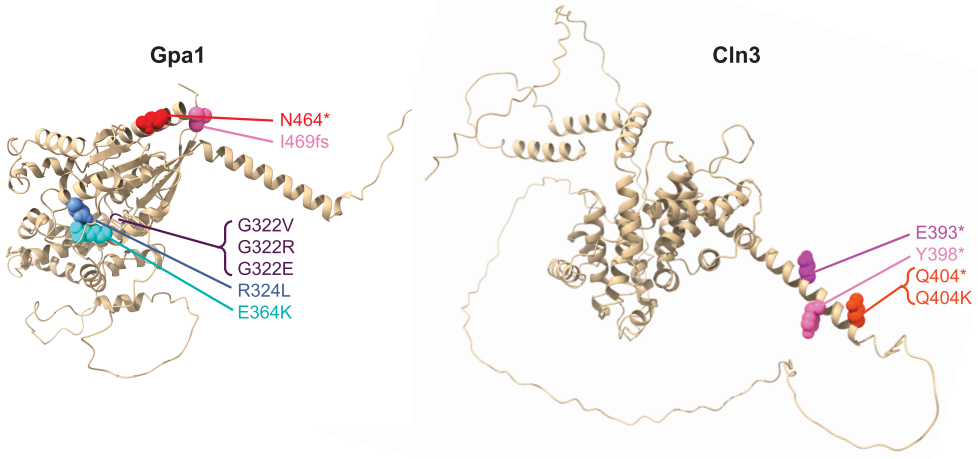


Fig. 3. Dominant mutations in Gpa1 and Cln3. The identity and patterns of mutations in *GPA1* and *CLN3* imply specific molecular mechanisms for dominant alpha-factor-resistant mutations. Dominant mutations in Gpa1 cluster in 2 regions: the GTP binding domain and the C-terminal domain that interacts with the Ste2 receptor. Dominant mutations in Cln3 arise in (or truncate) the C-terminal PEST domain. The structures were generated using UCSF ChimeraX.

mutations in this region modulate the strength of signaling through the mating pathway. Lysine-to-proline substitutions at positions 467 and 468, or a nonsense mutation at position 468, decrease mating ability and induced signaling through the mating pathway (Hirsch et al. 1991; Yvert et al. 2003). We identify a nonsense mutation at position 464 and a frameshift at position 469 that add 6 amino acids to the C-terminus of the protein (Fig. 3). These are likely gain-of-function mutations that interfere with release of the G protein from the Ste2 receptor, because loss of this interaction (for example by deletion of *GPA1*) would result in constitutive signaling through the pathway and a cell-cycle arrest in the absence of alpha-factor.

Another common target for dominant mutations is the G1 cyclin gene *CLN3*. All 4 dominant *CLN3* mutations affect the C-terminal PEST domain (Fig. 3). Mutations in this region are known to be hyperactive dominant alleles that shorten G1 and decrease alpha-factor sensitivity. One mutation changes Lys404 to Gln; and the other 3 remove the PEST domain. Interestingly, one truncation (Q404*) is identical to the original *cln3-1* allele (Nash et al. 1988). Loss of the PEST domain produces a more stable, hyperactive cyclin that promotes G1 to S progression (Cross and Blake 1993). Like the dominant *GPA1* mutants, our dominant *CLN3* mutants are not dominant negative, as null mutations of *CLN3* have the opposite phenotype from what we observe: prolonged G1 phase and sensitivity to alpha-factor (Teufel et al. 2019).

Dominant mutations in *STE4* are dominant negative

Ste4 is the Gβ subunit of the heterotrimeric G-protein. It is a WD40 domain-containing protein that adopts a canonical 7-blade beta-propeller structure (Fig. 4a). Over half of the dominant alpha-factor-resistant mutations (14/26) are found in the *STE4* gene. The 9 nonsense/frameshift and 5 missense mutations are distributed throughout the protein (Fig. 4b). Dominant missense mutations tend to be in phenotypic Cluster 3.A, whereas nonsense/frameshift tend to be Cluster 3.B (Figure 4c). Both Clusters 3.A and 3.B have basal and induced signaling through the mating pathway; however, Cluster 3.A is unable to mate (Fig. 2). In *STE4*, therefore, dominant missense mutations have more severe phenotypes than dominant nonsense/frameshift mutations, a pattern consistent with a dominant-negative mechanism in which a subset of missense mutations interfere with the function of the protein complex.

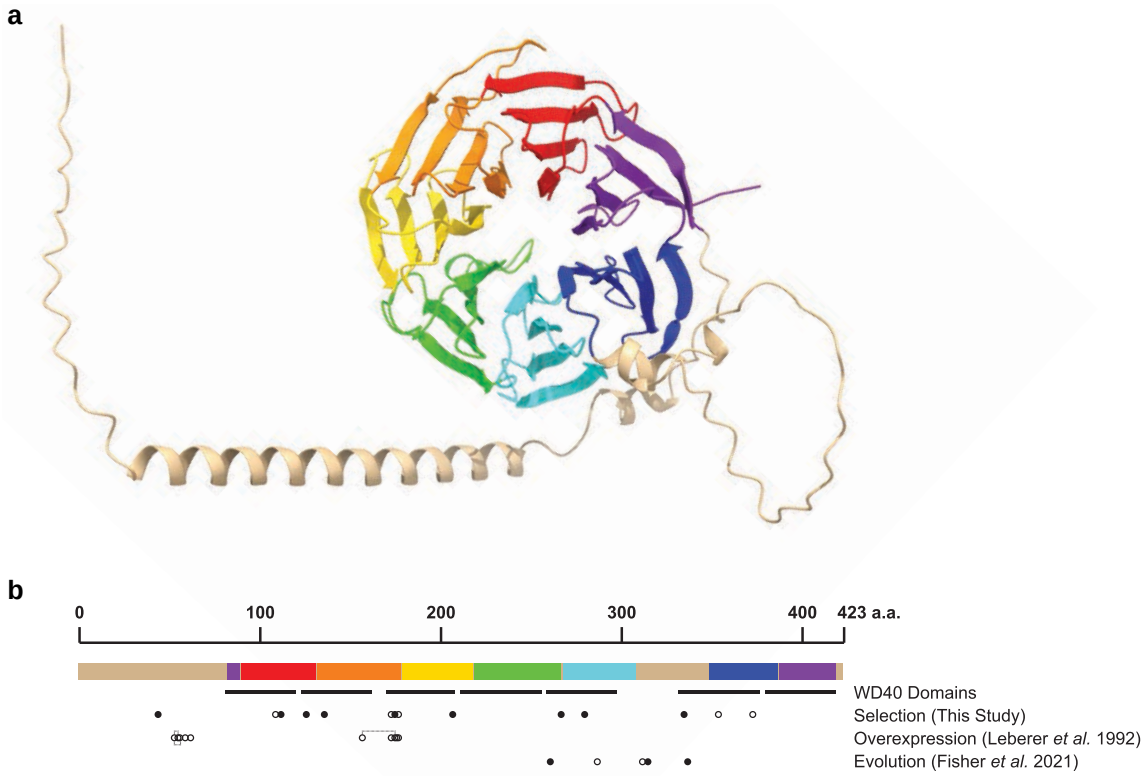
An earlier study overexpressed a mutagenized *STE4* library in a haploid strain to screen for dominant-negative mutations affecting alpha-factor resistance (Leberer et al. 1992). This study identified 9 dominant-negative missense mutations in Ste4, but unlike our results, they observed mutations in only 2 regions of the protein. Interestingly, we observe mutations at 2 of the residues found in this prior study: Val173 and Phe177. Both our results and Leberer et al. 1992 indicate that dominant-negative mutations in *STE4* have modest effects on other mating-associated phenotypes, including basal and induced expression of downstream reporters and mating ability.

The observation that *STE4* is a large target for alpha-factor-resistant mutations is consistent with our previous results from experimental evolution. Mutations that inactivate the mating pathway are common in laboratory evolution experiments and confer a fitness benefit due to elimination of the cost of basal gene expression (Lang et al. 2009). *MAT***a**/**a** autodiploids, like haploids, should benefit from mutations that inactivate the mating pathway. However, only *STE4* is identified as a common target of selection across the autodiploid populations (Fisher et al. 2018; Fisher et al. 2021).

Specific estimates of the fraction of mutations that are dominant suggest that the number is generally less than 10% (Wilkie 1994); although deep mutational scanning studies have shown that, in some cases, it can be as high as 30% (Padhy et al. 2023; Flynn et al. 2024). The fraction of new mutations that are genetically dominant is likely influenced by the protein structure, function, and abundance. By focusing on the output of a signal transduction pathway, our analysis averages across multiple genes in which dominant mutations could arise. Within the mating pathway, we find that 3 genes harbor a disproportionately large number of the dominant mutations, showing how the choice of a single gene could produce very different estimates of this fundamental genetic parameter. Our estimate that ~1% of beneficial mutations conferring alpha-factor resistance are dominant is broadly consistent with the genome-wide estimate that ~3% of yeast genes are haploinsufficient (Deutschbauer et al. 2005).

Dominant mutations in the yeast mating pathway are clustered in the Gα and the Gβ subunits of the heterotrimeric G-protein (Gpa1 and Ste4, respectively) as well as the G1-cyclin (Cln3). Mutations in *STE4* appear to be dominant negative, interfering with signaling. Mutations in *GPA1* and *CLN3* appear to be

Downloaded from https://academic.oup.com/genetics/advance-article/doi/10.1093/genetics/iyag105/8662036 by Lehigh University user on 28 May 2026



c

Background	Experiment	Clone ID	Mutation	Cluster	Reference
Diploid	Selection	C09	Gln44*	3.B	This study
Diploid	Selection	E09	Ser109Ile	3.A	This study
Diploid	Selection	H12	Gln112*	3.B	This study
Diploid	Selection	E11	Lys126fs	3.B	This study
Diploid	Selection	E08	Trp136*	3.A	This study
Diploid	Selection	E12	Val173Asp	3.A	This study
Diploid	Selection	C07	Ser175*	3.B	This study
Diploid	Selection	E07	Phe177Ser	3.A	This study
Diploid	Selection	C12	Trp207*	other	This study
Diploid	Selection	G12	Tyr267fs	3.B	This study
Diploid	Selection	H10	Lys280fs	3.B	This study
Diploid	Selection	C10	Ser335*	3.B	This study
Diploid	Selection	E10	Ser354Pro	3.A	This study
Diploid	Selection	F08	Cys373Trp	other	This study
Haploid+Plasmid	Overexpression	n/a	Gln52Lys/Lys55Asn	n/a	Leberer et al. 1992
Haploid+Plasmid	Overexpression	n/a	Gln52Arg/Ala56Val	n/a	Leberer et al. 1992
Haploid+Plasmid	Overexpression	n/a	Lys55Glu	n/a	Leberer et al. 1992
Haploid+Plasmid	Overexpression	n/a	Lys59Glu	n/a	Leberer et al. 1992
Haploid+Plasmid	Overexpression	n/a	Asp62Asn	n/a	Leberer et al. 1992
Haploid+Plasmid	Overexpression	n/a	Asn157His/Ser175Pro	n/a	Leberer et al. 1992
Haploid+Plasmid	Overexpression	n/a	Val173Gly	n/a	Leberer et al. 1992
Haploid+Plasmid	Overexpression	n/a	Ile176Asn	n/a	Leberer et al. 1992
Haploid+Plasmid	Overexpression	n/a	ΔPhe177	n/a	Leberer et al. 1992
Diploid	Evolution	n/a	Ser261fs	n/a	Fisher et al. 2021
Diploid	Evolution	n/a	Ala287Ser	n/a	Fisher et al. 2021
Diploid	Evolution	n/a	Arg312Gln	n/a	Fisher et al. 2021
Diploid	Evolution	n/a	Glu315*	n/a	Fisher et al. 2021
Diploid	Evolution	n/a	Gln337*	n/a	Fisher et al. 2021

Fig. 4. Dominant-negative mutations are distributed throughout the Ste4 protein. a) Ste4 is a WD40 domain-containing protein that adopts a 7-blade beta-propeller structure. The structure shown is the alpha-fold predicted structure with each blade indicated a different color. The structure was generated using UCSF ChimeraX. b) The primary structure of the Ste4 protein indicating the locations of the WD40 domains, and the dominant-negative missense (open circles) and nonsense/frameshift mutations (filled circles) from this study, as well as dominant-negative mutations from an overexpression study (Leberer et al. 1992) and from experimental evolution (Fisher et al. 2021). c) A list of dominant-negative Ste4 mutations from this study, Leberer et al. 1992, and Fisher et al. 2021.

dominant mutations that lock these proteins in a state that either prevents signaling through the pathway or allows for bypass of the pheromone-induced G1 arrest. Overall, our results shed light on the prevalence of dominant mutations and the mechanisms of genetic dominance.

Data availability

The short-read sequencing data reported in this study have been deposited to the NCBI BioProject database, accession number PRJNA1330868. Flow-cytometry measurements underlying Fig. 2

Downloaded from https://academic.oup.com/genetics/advance-article/doi/10.1093/genetics/iyag105/8662036 by Lehigh University user on 28 May 2026

are provided in Supplementary Table 1, and representative plate-based phenotypes are provided in Supplementary Fig. 2. Additional mutation and copy-number data are provided in Supplementary Dataset 1.

Supplemental material available at GENETICS online.

Acknowledgments

We thank members of the Lang Lab for comments on the manuscript.

Funding

This work was supported by grants from the National Institutes of Health (R35GM149540 and R01GM127420). We are grateful to the National Institutes of Health for an Administrative Supplement to Support Undergraduate Summer Research (R01GM127420-04S1). Portions of this research were conducted on Lehigh University's Research Computing infrastructure partially supported by the National Science Foundation (Award 2019035).

Conflicts of interest

None declared.

Author contributions

Conceptualization: GIL. Experiments: MGA, AAM, GIL. Analysis: MGA, GIL. Writing: GIL. Editing: GIL, AAM, MGA. Funding Acquisition: GIL.

Literature cited

Alvaro CG, Thorner J. 2016. Heterotrimeric G protein-coupled receptor signaling in yeast mating pheromone response. J Biol Chem. 291:7788–7795. https://doi.org/10.1074/jbc.R116.714980.

Bardwell L. 2005. A walk-through of the yeast mating pheromone response pathway. Peptides. 26:339–350. https://doi.org/10.1016/j.peptides.2004.10.002.

Boeva V *et al.* 2012. Control-FREEC: a tool for assessing copy number and allelic content using next-generation sequencing data. Bioinformatics. 28:423–425. https://doi.org/10.1093/bioinformatics/btr670.

Bolger AM, Lohse M, Usadel B. 2014. Trimmomatic: a flexible trimmer for Illumina sequence data. Bioinformatics. 30:2114–2120. https://doi.org/10.1093/bioinformatics/btu170.

Cingolani P *et al.* 2012. A program for annotating and predicting the effects of single nucleotide polymorphisms, SnpEff: SNPs in the genome of *Drosophila melanogaster* strain w1118; iso-2; iso-3. Fly (Austin). 6:80–92. https://doi.org/10.4161/fly.19695.

Colomina N, Garí E, Gallego C, Herrero E, Aldea M. 1999. G1 cyclins block the Ime1 pathway to make mitosis and meiosis incompatible in budding yeast. EMBO J. 18:320–329. https://doi.org/10.1093/emboj/18.2.320.

Cross FR, Blake CM. 1993. The yeast Cln3 protein is an unstable activator of Cdc28. Mol Cell Biol. 13:3266–3271. https://doi.org/10.1128/mcb.13.6.3266-3271.1993.

Deutschbauer AM *et al.* 2005. Mechanisms of haploinsufficiency revealed by genome-wide profiling in yeast. Genetics. 169:1915–1925. https://doi.org/10.1534/genetics.104.036871.

Fisher KJ, Buskirk SW, Vignogna RC, Marad DA, Lang GI. 2018. Adaptive genome duplication affects patterns of molecular evolution in *Saccharomyces cerevisiae*. PLoS Genet. 14:e1007396. https://doi.org/10.1371/journal.pgen.1007396.

Fisher KJ, Vignogna RC, Lang GI. 2021. Overdominant mutations restrict adaptive loss of heterozygosity at linked loci. Genome Biol Evol. 13:evab181. https://doi.org/10.1093/gbe/evab181.

Flynn JM, Joyce ME, Bolon DNA. 2024. Dominant negative mutations in yeast Hsp90 reveal triage decision mechanism targeting client proteins for degradation [preprint]. bioRxiv 573950. https://doi.org/10.1101/2024.01.02.573950.

Garrison E, Marth G. 2012. Haplotype-based variant detection from short-read sequencing [preprint], arXiv, arXiv:1207.3907. https://doi.org/10.48550/arXiv.1207.3907.

Hartwell LH. 1980. Mutants of *Saccharomyces cerevisiae* unresponsive to cell division control by polypeptide mating hormone. J Cell Biol. 85:811–822. https://doi.org/10.1083/jcb.85.3.811.

Herskowitz I. 1995. MAP kinase pathways in yeast: for mating and more. Cell. 80:187–197. https://doi.org/10.1016/0092-8674(95)90402-6.

Hicks JB, Herskowitz I. 1976. Interconversion of yeast mating types I. Direct observations of the action of the homothallism (HO) gene. Genetics. 83:245–258. https://doi.org/10.1093/genetics/83.2.245.

Hirsch J, Dietzel C, Kurjan J. 1991. The carboxyl terminus of Scg1, the G alpha subunit involved in yeast mating, is implicated in interactions with the pheromone receptors. Genes Dev. 5:467–474. https://doi.org/10.1101/gad.5.3.467.

Ho CH *et al.* 2009. A molecular barcoded yeast ORF library enables mode-of-action analysis of bioactive compounds. Nat Biotechnol. 27:369–377. https://doi.org/10.1038/nbt.1534.

Knight KM *et al.* 2021. A universal allosteric mechanism for G protein activation. Mol Cell. 81:1384–1396. e1386. https://doi.org/10.1016/j.molcel.2021.02.002.

Lang GI. 2018. Measuring mutation rates using the Luria-Delbrück fluctuation assay. In: Muzi-Falconi M, Brown GW, editors. Genome instability: methods and protocols. Springer New York. p. 21–31.

Lang GI, Murray AW. 2008. Estimating the per-base-pair mutation rate in the yeast *Saccharomyces cerevisiae*. Genetics. 178:67–82. https://doi.org/10.1534/genetics.107.071506.

Lang GI, Murray AW, Botstein D. 2009. The cost of gene expression underlies a fitness trade-off in yeast. Proc Natl Acad Sci U S A. 106:5755–5760. https://doi.org/10.1073/pnas.0901620106.

Leberer E, Dignard D, Hougan L, Thomas DY, Whiteway M. 1992. Dominant-negative mutants of a yeast G-protein beta subunit identify two functional regions involved in pheromone signalling. EMBO J. 11:4805–4813. https://doi.org/10.1002/j.1460-2075.1992.tb05586.x.

Li H, Durbin R. 2009. Fast and accurate short read alignment with Burrows–Wheeler transform. Bioinformatics. 25:1754–1760. https://doi.org/10.1093/bioinformatics/btp324.

Mackay V, Manney TR. 1974a. Mutations affecting sexual conjugation and related processes in *Saccharomyces cerevisiae*. I. Isolation and phenotypic characterization of nonmating mutants. Genetics. 76:255–271. https://doi.org/10.1093/genetics/76.2.255.

Mackay V, Manney TR. 1974b. Mutations affecting sexual conjugation and related processes in *Saccharomyces cerevisiae*. II. Genetic analysis of nonmating mutants. Genetics. 76:273–288. https://doi.org/10.1093/genetics/76.2.273.

Manney TR, Woods V. 1976. Mutants of *Saccharomyces cerevisiae* resistant to the α mating-type factor. Genetics. 82:639–644. https://doi.org/10.1093/genetics/82.4.639.

Marad DA, Buskirk SW, Lang GI. 2018. Altered access to beneficial mutations slows adaptation and biases fixed mutations in diploids. Nat Ecol Evol. 2:882–889. https://doi.org/10.1038/s41559-018-0503-9.

Downloaded from https://academic.oup.com/genetics/advance-article/doi/10.1093/genetics/iyag105/8662036 by Lehigh University user on 28 May 2026

Matheson K, Parsons L, Gammie A. 2017. Whole-genome sequence and variant analysis of W303, a widely-used strain of *Saccharomyces cerevisiae*. G3 (Bethesda). 7:2219–2226. https://doi.org/10.1534/g3.117.040022.

Nash R, Tokiwa G, Anand S, Erickson K, Futcher A. 1988. The WHI1 + gene of *Saccharomyces cerevisiae* tethers cell division to cell size and is a cyclin homolog. EMBO J. 7:4335–4346. https://doi.org/10.1002/j.1460-2075.1988.tb03332.x.

Padhy AA, Mavor D, Sahoo S, Bolon DNA, Mishra P. 2023. Systematic profiling of dominant ubiquitin variants reveals key functional nodes contributing to evolutionary selection. Cell Rep. 42:113064. https://doi.org/10.1016/j.celrep.2023.113064.

Rosche WA, Foster PL. 2000. Determining mutation rates in bacterial populations. Methods. 20:4–17. https://doi.org/10.1006/meth.1999.0901.

Sarkar S, Ma WT, Sandri GH. 1992. On fluctuation analysis: a new, simple and efficient method for computing the expected number of mutants. Genetica. 85:173–179. https://doi.org/10.1007/BF00120324.

Strathern JN, Herskowitz I. 1979. Asymmetry and directionality in production of new cell types during clonal growth: the switching pattern of homothallic yeast. Cell. 17:371–381. https://doi.org/10.1016/0092-8674(79)90163-6.

Teufel L *et al.* 2019. A transcriptome-wide analysis deciphers distinct roles of G1 cyclins in temporal organization of the yeast cell cycle. Sci Rep. 9:3343. https://doi.org/10.1038/s41598-019-39850-7.

Velazhahan V *et al.* 2021. Structure of the class D GPCR Ste2 dimer coupled to two G proteins. Nature. 589:148–153. https://doi.org/10.1038/s41586-020-2994-1.

Wilkie AO. 1994. The molecular basis of genetic dominance. J Med Genet. 31:89–98. https://doi.org/10.1136/jmg.31.2.89.

Wu Y-L, Hooks SB, Harden TK, Dohlman HG. 2004. Dominant-negative inhibition of pheromone receptor signaling by a single point mutation in the G protein alpha subunit. J Biol Chem. 279:35287–35297. https://doi.org/10.1074/jbc.M404896200.

Yvert G *et al.* 2003. Trans-acting regulatory variation in *Saccharomyces cerevisiae* and the role of transcription factors. Nat Genet. 35:57–64. https://doi.org/10.1038/ng1222.

Editor: P. Magwene

Downloaded from https://academic.oup.com/genetics/advance-article/doi/10.1093/genetics/iyag105/8662036 by Lehigh University user on 28 May 2026